On the performance of non-coherent CFAR detectors in sea-clutter: A comparison study

Zakia Terki, Amar Mezache and Fouad Chebbara

Abstract—**In radar systems, detection performance depends on assumed target and clutter statistical distributions. The probability of detection is shown to be sensitive to the degree of estimation accuracy of clutter levels. In this work, the performances of non-coherent logt-CFAR, zlog(z)-CFAR and Bayesian-CFAR detectors are investigated using both simulated and real data. Three clutter disturbances are considered named log-normal, Weibull and Pareto type II. Based on simulated data, existing CFAR algorithms provide fully CFAR decision rules. From IPIX real data, the dependence of the false alarm probability associated to each detector is studied. With different range resolutions, it is shown that the Bayesian-CFAR algorithm exhibits a small deviation of the false alarm probability.**

***Index Terms*—Radar, Sea-clutter, logt-CFAR, zlog(z)-CFAR, Pareto type II model, Bayesian-CFAR.**

I. Introduction

The detection performance of maritime radars is restricted by the unwanted sea-echo or clutter [1]. Radar clutter modeling is a serious research issue in the field of targets detection and track applications. Although the number of these target-like data is small, they may cause false alarm and perturb the target detection. Reliable radar signal processing algorithms including CFAR (constant false alarm rate) detectors are constructed on the basis of the best selection of background clutter model [2]. Development of radar systems encourages researchers to use theoretical heavy tailed probability density functions (pdf) that are found in the open literature of statistics and mathematics. Nowadays, the Rayleigh distribution becomes a special case of some sea reverberation data, because there is a restriction of the application of a central limit theorem.

Submitted: 01May 2021.

Amar Mezache is with Département d'Electronique, Université Mohamed Boudiaf Msila, Algérie
Laboratoire SISCOM, Université de Constantine
Email: amar.mezache@univ-msila.dz

Zakia Terki and Fouad Chebbara are with Laboratoire de Génie Electrique, LAGE, Département d'Electronique, Université Kasdi Merbah Ouargla, Algérie.

The two parameters log-normal, Weibull, *K* and Pareto laws have been offered as models for the amplitude of both land and sea-clutter [2-4]. More recently, compound distribution with trimodal discrete texture law has been added to yield a fairly good description of empirical data [5]. Adaptive CFAR detectors are developed to overcome the increase of the false alarm number due to the use of conventional detectors with fixed thresholds. Moreover, if wrong clutter model or inappropriate clutter level estimator is used, such false alarm problem can not be resolved [6]. In reality, the phenomenon complexity of radiation scattered from turbulent or rough surface and the lack of explicit solutions of underling algorithms have also a negative impact on the development of optimal CFAR detectors.

In terms of sea-clutter model type, several authors have considered different decision rules that are independent of true clutter parameters [7-9]. From [3], the logt-CFAR maintains the CFAR property if independent radar returns follow log-normal or Weibull population. Recently, Gouri *et al* proposed in [7] the zlog(z)-CFAR detector for Weibull background. This procedure provides similar results with respect to the well known ML-CFAR algorithm given in [4], but with a small computation time. Some CFAR detectors operating in homogeneous and heterogeneous Pareto type II clutter are presented when the shape parameter or the scale parameter of the Pareto type II model is known a priori [8]. If these parameters are unknown, an alternative procedure based upon the Bayesian approach is introduced in which a modified decision rule is obtained in integral form [9].

In summary, we observe that the previous work based on the Bayesian framework did not show performances comparisons between the Bayesian-CFAR detector with their corresponding logt-CFAR and zlog(z)-CFAR detectors using real data. In this work, the clutter is assumed to be log-normal, Weibull or Pareto type II distributed. The dependence of the false alarm probability is presented. From simulated data, CFAR detectors provide fully CFAR decision rules. From IPIX (Intelligent Pixel processing X-band) real data with different range resolutions, it is shown that the Bayesian-

CFAR algorithm exhibits a small deviation of the false alarm probability.

The paper is organized as follows. Section 2 summarizes three statistical distributions characterizing radar sea echoes. In Section 3, full CFAR detectors related to the log-normal, Weibull and Pareto type II distributions are given. After giving partial CFAR detectors in Pareto type II clutter in Section 4, detection performances of underling CFAR algorithms are then compared. Finally, main conclusions are outlined in Section 5.

II. SEA-CLUTTER MODELS

In modern high resolution radar, the clutter (sea-clutter, weather clutter or land clutter) returns may not follow the Rayleigh model, since the amplitude distribution develops a "larger" tail that may increase the false alarm rate. As an alternative, compound Gaussian distributions have been studied to fit sea radar clutter [7]. In the following, three popular distributions that are considered for maritime targets CFAR detection are presented.

A. Log-normal model

The log-normal distribution best describes land clutter at low grazing angles. It also fits sea-clutter in the plateau region [3, 10]. The pdf of the amplitude X is

$$p(x) = \frac{1}{\sigma x\sqrt{2\pi}} \exp\left(-\frac{(ln(x) - \mu)^2}{2\sigma^2} \right) , \; x > 0 \quad (1)$$

where μ and σ are the median and the standard deviation of the random variable ln(x) respectively.

B. Weibull model

The Weibull pdf is used to model sea-clutter at low grazing angles (less than five degrees) for propagation frequencies vary between 1 and 10GHz. It is determined by the slope parameter a and a median scatter coefficient $\overline{\sigma}_0$, and is given by [4, 10].

$$p(x) = \frac{c}{b}\left(\frac{x}{b}\right)^{c-1} \exp\left(-\left(\frac{x}{b}\right)^{c} \right), \; x > 0 \quad (2)$$

where c=1/a is the shape parameter and $b = \overline{\sigma}_0^{1/c}$ is the scale parameter.

C. Pareto type II model

The Pareto disturbance is considered as a possible model to analyze data sets with very heavy tail, such as sea-clutter measurements that have heavy tail. The Pareto type II pdf is obtained if the texture component follows the inverse gamma law [8, 9]. The latter describes the variations of the local reflected power due to the tilting of the illuminated area. The statistics of a Pareto distributed random variable x have been described in [8] by the probability density function as

$$p(x) = \frac{\alpha\beta^{\alpha}}{(x+\beta)^{\alpha+1}}, \; x > 0 \quad (3)$$

where α is the shape parameter and β the scale parameter. For high resolution sea clutters, the shape parameter α is typically in the range $2.1 \leq \alpha \leq \infty$, where α close to 2.1 represents a very spiky clutter and $\alpha \to \infty$ corresponds to thermal noise (Rayleigh clutter).

III. RELATED CFAR DETECTORS

Radar target detection is usually modeled by binary hypothesis test. The observed signal y under the two hypotheses, H_1 for target present and H_0 for target absent (clutter only), is given by

$$\begin{cases} H_1 : \; y = s + c \\ H_0 : \; y = \quad c \end{cases} \quad (4)$$

where y, s and c are complex numbers.

A. Logt-CFAR detector

The decision rule associated to this detection procedure is independent of true values of the clutter model parameters and is suitable for log-normal or Weibull background [3]. The test is

$$\log(X_0) \underset{H_0}{\overset{H_1}{\gtrless}} \hat{\mu} + \tau\hat{\sigma} \quad (5)$$

where $X_0 = |y|$ is the magnitude of the cell under test (CUT), τ is the threshold multiplier, $\hat{\mu}$ and $\hat{\sigma}$ are the estimated mean and standard deviation of the random variable log(X).

B. zlog(z)-CFAR detector

The forthcoming adaptive threshold is also given as a function of estimated shape and scale parameters of Weibull clutter. The coefficient τ is used to fix the desired value of the false alarm probability, P_{FA}

$$X_0 = \hat{b}\,\tau^{1/\hat{c}} \quad (6)$$

From [7], $\hat{c}$ and $\hat{b}$ are obtained by a flexible approach based on the interpolation method

$$\begin{cases} \dfrac{\langle x \ln x \rangle}{\langle x \rangle} - \langle \ln x \rangle - 1 = \dfrac{1}{\hat{c}} \left(\psi(1/\hat{c}) - \psi(1) \right) \\ \hat{b} = \left(\dfrac{1}{N} \sum_{i=1}^{M} (x_i)^{\hat{c}} \right)^{1/\hat{c}} \end{cases} \tag{7}$$

where N is the size of the CRP (clutter range profile) and $\psi(.)$ the Psi (digamma) function.

C. Bayesian-CFAR detector

The Bayesian method is one of the best techniques for obtaining decision rules with a CFAR property. This method provides the flexibility of extracting the posterior decision rule from its respective posterior distribution. It is considered here for the case in which both Pareto type II parameters in (3) are unknown. According to [9], the Bayesian based CFAR detector is constructed by means of steps below:

Step 1: Calculate the natural logarithm of (3).

Step 2: Determine the Fisher information matrix.

Step 3: Calculate the Jeffreys prior distribution.

Step 4: Obtain the joint density of the CRP.

Step 5: Calculate the joint density of the Pareto distributional parameters, conditioned on the CRP.

Step 6: Calculate the Bayes predictive density.

Step 7: Calculate the P_{FA} expression as a function of the threshold τ and samples, X_i, i=1, …N.

To compute the P_{FA}, triple integrals are considered [9]. Hence

$$P_{FA} = \int_{\tau}^{\infty} \int_{0}^{\infty} \int_{0}^{\infty} f\left(x_0 | \alpha, \beta\right) f\left(\alpha, \beta | x_1, x_2, \ldots, x_N\right) f(\alpha, \beta) d\alpha d\beta dx_0 \tag{8}$$

where $f\left(z_0 | \alpha, \beta\right)$ is the density of the CUT conditioned on the clutter parameters, $f\left(\alpha, \beta | x_1, x_2, \ldots, x_N\right)$ is the posterior density of the parameters α and β conditioned on the CRP and $f(\alpha, \beta)$ is the prior distributions of the clutter parameters. From [9], it is demonstrated that the P_{FA} is independent of α and β.

$$P_{FA} = \frac{\displaystyle\int_0^{\infty} \frac{\phi^{N-1}}{\displaystyle\prod_{i=1}^{N} (\phi x_i + 1)} \left[\log(\tau\phi + 1) + \sum_{i=1}^{N} \log(\phi x_i + 1) \right]^{-N} d\phi}{\displaystyle\int_0^{\infty} \frac{\phi^{N-1}}{\displaystyle\prod_{i=1}^{N} (\phi x_i + 1)} \left[\sum_{i=1}^{N} \log(\phi x_i + 1) \right]^{-N} d\phi} \tag{9}$$

Consequently, one can conclude that the Bayesian test is to reject H_0 if the following test statistic is negative [9]. From (9), τ is replaced by X_0 and he threshold is obtained numerically as

$$\begin{aligned} T(x_1, x_2, \ldots, x_N) = & \int_0^{\infty} \frac{\phi^{N-1}}{\displaystyle\prod_{i=1}^{N} (\phi x_i + 1)} \\ & x \left[\left[\log(\phi x_0 + 1) + \sum_{i=1}^{N} \log(\phi x_i + 1) \right]^{-N} \right. \\ & \left. - P_{FA} \left[\sum_{i=1}^{N} \log(\phi x_i + 1) \right]^{-N} \right] d\phi \end{aligned} \tag{10}$$

The decision rule can also be written in the form

$$-T(z_1, z_2, \ldots, z_N) \underset{H_0}{\overset{H_1}{\gtrless}} 0 \tag{11}$$

IV. DETECTION COMPARISONS

In this section, we conduct firstly several Monte-Carlo simulations as well as IPIX real data in order to evaluate the detection performance and the false alarm properties of CFAR detectors given in [3, 4, 7-9]. For instance, the target of interest fluctuates according to Swerling 1 model. For comparison purposes, three partial CFAR detectors are considered for simulated data [8].

A. Partial GM-CFAR detector (known β)

Under the assumption of iid (independent and identically distributed) Pareto type II distributed samples, the decision rule of the GM-CFAR (geometric mean-CFAR) detector is given in terms of β

$$X_0 \underset{H_0}{\overset{H_1}{\gtrless}} \beta \left(\prod_{i=1}^{N} \left(1 + \frac{X_i}{\beta} \right)^{\tau} - 1 \right) \tag{12}$$

where $\tau = P_{FA}^{-1/N} - 1$ and the corresponding P_{FA} yields

$$P_{FA} = (1 + \tau)^{-N} \tag{13}$$

B. Partial OS-CFAR detector (known β)

In the presence of outliers, the output of the reference window are sorted in increasing order. The k^{th} order statistic $X_{(k)}$ is chosen to estimate the clutter power. From [8], one concludes that the resulting OS-CFAR (order statistic-CFAR) detector is also dependent of β

$$X_0 \underset{H_0}{\overset{H_1}{\gtrless}} \beta\left(\left(1+\frac{X_{(k)}}{\beta}\right)^{\tau}-1\right) \tag{14}$$

Here, the equivalent P_{FA} formula is

$$P_{FA}=\frac{N!}{(N-k)!}\frac{\Gamma(N-k+\tau+1)}{\Gamma(N+\tau+1)} \tag{15}$$

Where τ is computed numerically.

C. Partial OS-CFAR detector (known α)

In this case, the decision rule for known α is given by [8]

$$X_0 \underset{H_0}{\overset{H_1}{\gtrless}} \tau X_{(k)} \tag{16}$$

where τ is determined via numerical inversion of P_{FA} [8]

$$P_{FA}=k\binom{N}{k}\int_0^1 (1-\phi)^{k-1}\phi^{N-k}\left(1+\tau\left(\phi^{\frac{1}{\alpha}}-1\right)\right)^{-\alpha} d\phi \tag{17}$$

D. Ideal detector (known α and β)

In order to provide an upper bound on detector performance, a linear detector with fixed threshold is considered

$$X_0 \underset{H_0}{\overset{H_1}{\gtrless}} \beta\left(P_{FA}\right)^{-\frac{1}{\alpha}}-\beta \tag{18}$$

E. Detection using simulated data

In this subsection, simulated Pareto type II clutter is considered to examine CFAR detectors given by (12), (14), (16) and (18). To do this, N+1 samples are generated by means of the following Matlab function.

$$X=\beta exp\left(exprnd\left(\frac{1}{\alpha},n,N+1\right)\right)-\beta \tag{19}$$

In the forthcoming outcomes, detectors (14) and (16) are denoted by OS-CFAR1 and OS-CFAR2 respectively. Figure. 1 depicts P_D values against the *SCR* (signal-to-clutter ratio) for N = 16, k=3N/4, $\alpha=2.7241$ and $\beta=\alpha-1$. As expected, the Bayesian-CFAR detector exhibits the lowest detection performance, because the two parameters are unknown which provide an error for clutter level estimates. If N = 32, the performances of all detectors are increased and the Bayesian-CFAR detector has always minimum P_D values as shown in Figure. 2. To illustrate the performance comparisons against interfering targets situation, we insert in leading and lagging windows two secondary targets with *ICR* = 5dB (Interfering-to-clutter ratio) for N = 16 as presented in Figure. 3. The degradation of GM-CFAR and Bayesian-CFAR detectors is remarkable. If two strong interfering targets with *ICR* = 10dB are injected in the CRP which creates non-homogeneous clutter, the Bayesian-CFAR detector offers also worst results as shown in Figure. 4. These attenuations in P_D values are due to the estimation errors of the clutter power in the CUT from non-identically distributed samples.

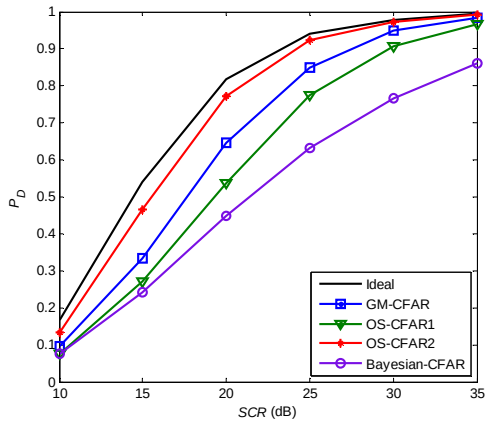

Figure. 1 P_D versus *SCR* of CFAR algorithms in Pareto type II clutter with N = 16, k=3N/4, $P_{FA}=10^{-3}$, $\alpha=2.7241$ and $\beta=\alpha-1$.

F. Detection using real data

The IPIX real data is now used to illustrate the P_{FA} values in terms of the threshold scale factor, range resolutions and antennas polarizations. IPIX is experimental X-band search radar, capable of dual polarized and frequency agile operation. We focus our analysis on the datasets 84, 85 and 86 which correspond to the range resolutions 30m, 15m and 3m respectively. Characteristic features of the IPIX radar are given in [11]. In this part, the magnitude (envelop) of real data is used as the input of each detector.

For cases of HH polarization, range resolutions of 3m, 15m and 30m with a linear detector, Figure. 5 presents three curves of P_{FA} values against the scale

factor, τ. Here, thresholds given by (5) and (6) are used. Clearly, the CFAR property is not maintained in terms of range resolutions. This implies that log-normal and Weibull distributions have not the ability to fit IPIX data for different range resolutions. If the Bayesian-CFAR is applied to these scenarios of the data, resulting P_{FA} values are comparable as depicted in Figure. 6. Thus, one concludes that the Pareto type II is well suited for IPIX data. Now we change the antennas polarization to be VV. Figure. 7 highlights also the deviation of the P_{FA} if detectors (5) and (6) are used. In this study, Figure. 8 shows also the best approximation of the P_{FA} values within the use of Bayesian decision rule given by (11).

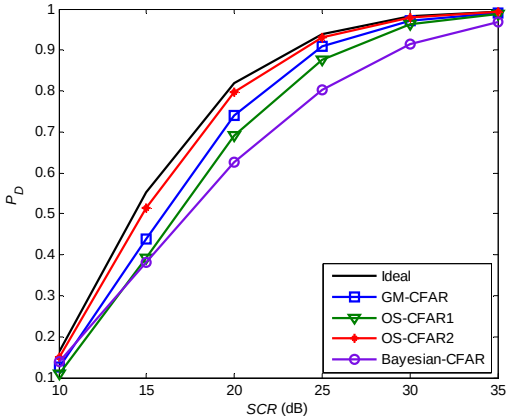

Figure. 2 P_D versus SCR of CFAR algorithms in Pareto type II clutter with N = 32, k = 3N/4, P_{FA} = 10^{-3}, $\alpha = 2.7241$ and $\beta = \alpha - 1$.

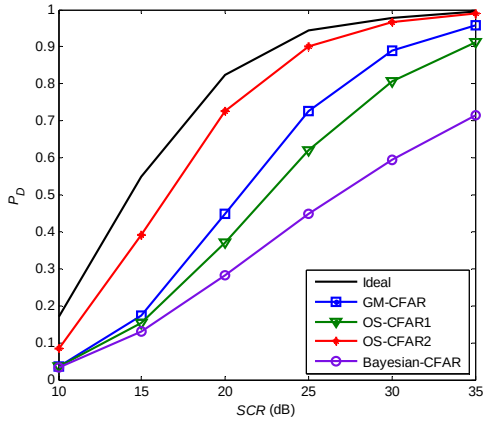

Figure. 4 P_D versus SCR of CFAR algorithms in Pareto type II clutter and 2 interfering targets with ICR = 10dB, N = 16, k=3N/4, P_{FA} = 10^{-3}, $\alpha = 2.7241$ and $\beta = \alpha - 1$.

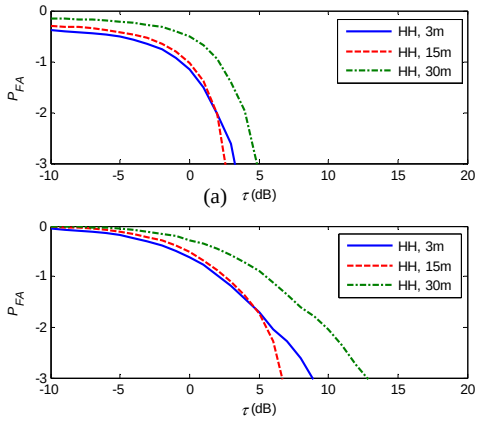

Figure. 5 P_{FA} versus scale factor τ of CFAR algorithms using IPIX data for HH polarization and N = 32

(a) logt-CFAR (log-normal or Weibull clutter case)
(b) zlogz-CFAR (Weibull clutter case)

Figure. 3 P_D versus SCR of CFAR algorithms in Pareto type II clutter and 2 interfering targets with ICR = 5dB, N = 16, k=3N/4, P_{FA} = 10^{-3}, $\alpha = 2.7241$ and $\beta = \alpha - 1$.

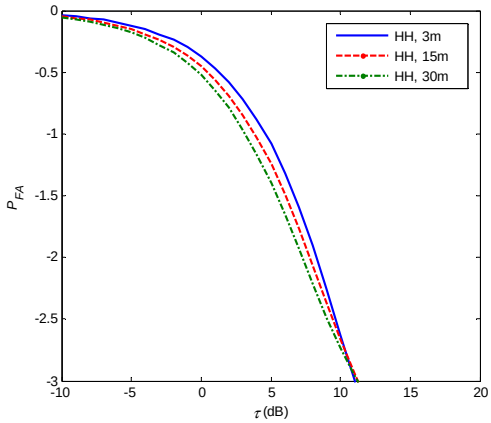

Figure. 6 P_{FA} versus detection threshold τ of Bayesian-CFAR detector (Pareto type II clutter case) using IPIX data for HH polarization and N = 32

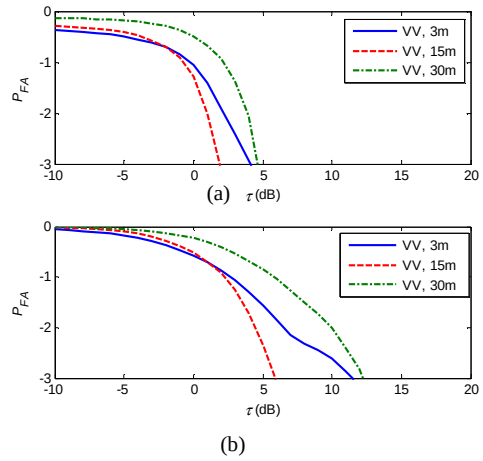

Figure. 7 P_{FA} versus scale factor τ of CFAR algorithms using IPIX data for VV polarization and $N = 32$
(a) logt-CFAR (log-normal or Weibull clutter case)
(b) zlogz-CFAR (Weibull clutter case)

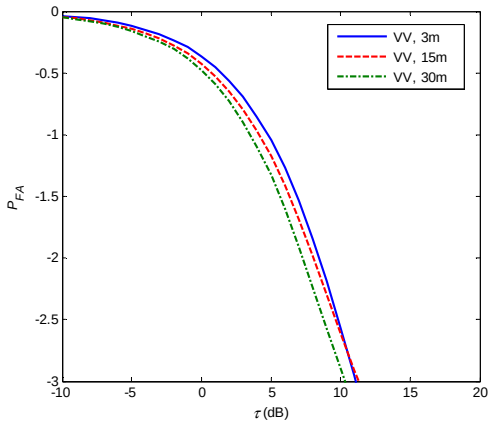

Figure. 8 P_{FA} versus detection threshold τ of Bayesian-CFAR detector (Pareto type II clutter case)
using IPIX data for VV polarization and $N = 32$

For HH and VV polarizations and a range resolution of 3m, the CFAR properties of zlogz-CFAR and logt-CFAR detectors are also checked as shown in Figures. 9 and 10. In this case, a data matrix of samples 10000x33 is used to estimate the P_{FA} in terms of τ. It is remarkable in these results that the P_{FA} curves are not converged at $P_{FA} = 10^{-3}$. This implies that such data does not fit precisely the Weibull or the lognormal disturbance.
In order to depict the P_D values, the mean of the scale factor of each detector is obtained to be $\tau = 3.5$ dB for the case of zlogz-CFAR algorithm and $\tau = 10$ for the case of logt-CFAR algorithm. As shown in Figure. 11, the logt-CFAR provides the best P_D results if HH polarization and a resolution of 3m are considered. When the VV polarization and a resolution of 3m are taken into account as shown in Figure. 12, the P_D values are almost overlapped. In this study, the logt-CFAR detector is preferred than the zloz-CFAR detector.

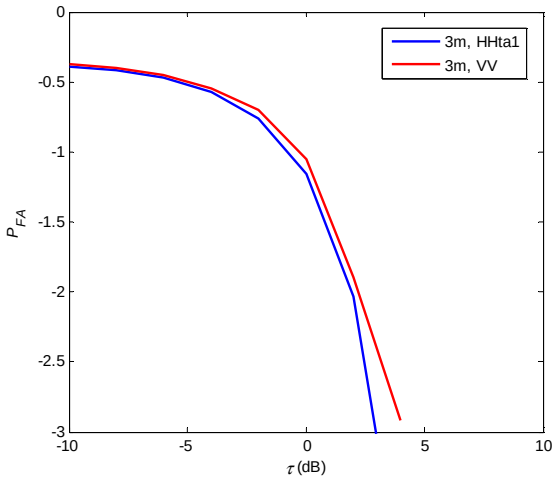

Figure. 9 P_{FA} versus scale factor τ of zlogz-CFAR algorithm for a resolution of 3m , HH and VV polarization.

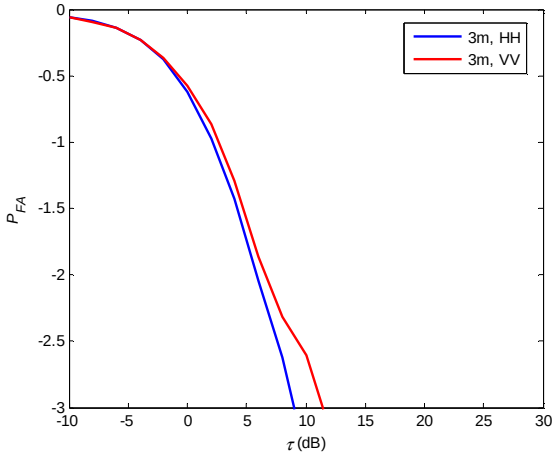

Figure. 10 P_{FA} versus scale factor τ of logt-CFAR algorithm for a resolution of 3m , HH and VV polarization.

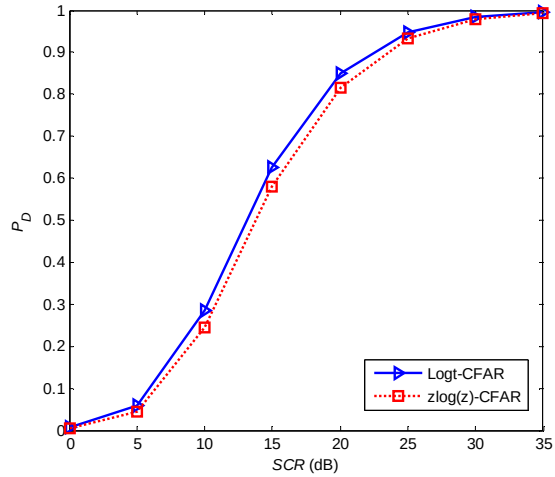

Figure. 11 P_D versus SCR of zlogz-CFAR and logt-CFAR algorithms using real data with HH polarization and 3m

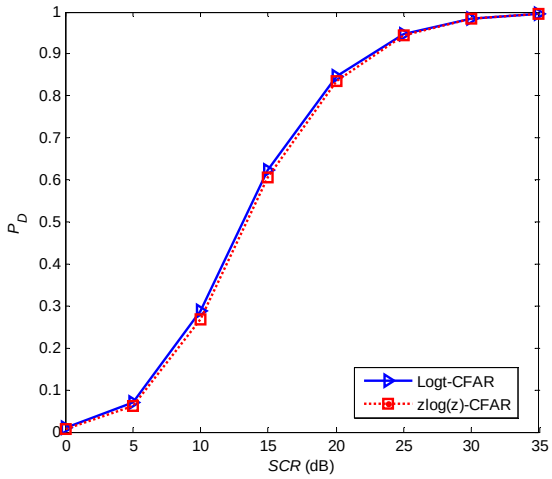

Figure. 12 P_D versus SCR of zlogz-CFAR and logt-CFAR algorithms using real data with VV polarization and 3m

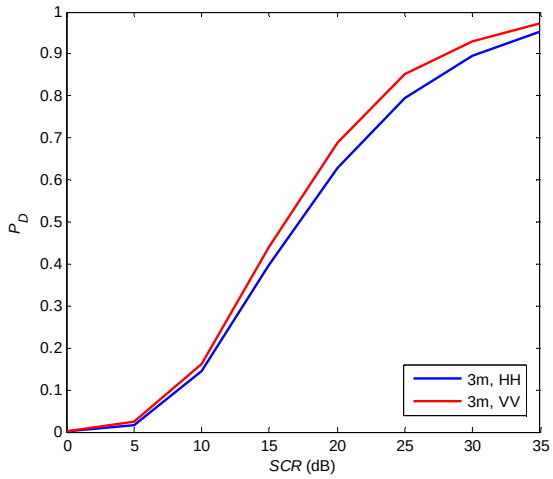

Figure. 14 P_D versus SCR of B-CFAR algorith using real data with HH and VV polarizations and resolution of 3m

For the case of a square law detector, the P_{FA} values related to the Bayesian-CFAR algorithm are computed for HH and VV polarizations and a resolution of 3m. It noticed in Figure. 13 that the P_{FA} curves are approximated, but the fitting error at $P_{FA} = 10^{-3}$ remains remarkable. The scale factor in this case is $\tau = 18$ dB. Figure. 14 sketchs the P_D in terms of the SCR using both HH and VV polarizations data with a resolution of 3m. The two curves have natures of monotonic increasing functions, but for the VV polarization case data the Bayesian-CFAR detector has better detection performances.

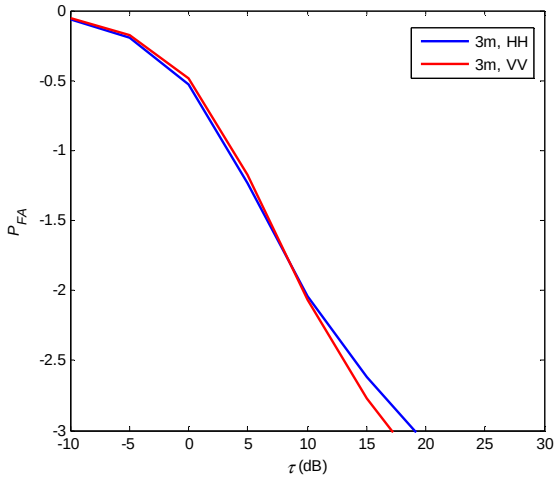

Figure. 13 P_{FA} versus scale factor τ B-CFAR algorithm for a resolution of 3m , HH and VV polarization.

V. Conclusions

In this work, we analyzed and compared the performance of non-parametric CFAR detectors in presence of log-normal, Weibull and Pareto type II clutter. From simulated data, the Bayesian-CFAR detector provided a full CFAR property and offered the smallest detection probability values, since the two parameters are unknown which make errors for the estimation of the clutter power. In terms of different range resolutions of IPIX real data, CFAR properties of zlogz-CFAR, logt-CFAR and Bayesian-CFAR detectors are studied almost the same false alarm probabilities were obtained using the Bayesian-CFAR detector for different resolutions 3m, 15m and 30m (envelop detector is used) and for a resolution of 3m (square law detector is used). It was also shown that logt-CFAR and zlog(z) CFAR algorithms can not ensure the CFAR property at the desired false alarm probability if the range cell resolution is changed.

References

[1] A. Davari, M. H. Marhaban, S. B. M. Noor, M. Karimadini, A. Karimoddini, “Parameter estimation of *K*-distributed sea clutter based on fuzzy inference and Gustafson–Kessel clustering”, Fuzzy Sets and Systems 163 (2011) 45–53.

[2] L. J. Marier, “Correlated K-distributed clutter generation for radar detction and track”, IEEE Transactions on Aerospace and Electronic Systems, Vol. 31, n°. 2, pp. 568-580, 1995.

[3] G. B. Goldstein, “False-alarm regulation in log-normal and Weibull clutter.” IEEE Transactions on Aerospace and Electronic Systems, AES-9 (1), pp. 84–92, 1973.

[4] R. Ravid and N. Levanon. “Maximum-likelihood CFAR for Weibull Background”, IEE Proceedings- F 139 (3), pp. 256–264, 1992.

[5] S. Bocquet, L. Rosenberg and C.H. Gierull, “Parameter estimation for a compound radar clutter model with trimodal discrete texture”, IEEE Transaction on Geosciences and Remote Sensing, published 25 March 2020.

[6] T. Laroussi and M. Barkat, “Performance analysis of order-statistic CFAR detectors in time diversity systems for partially correlated chi-square targets and multiple target situations: A comparison”, Journal of Signal Processing, Vol. 86, pp. 1617-1631, 2006.

[7] A. Gouri, A. Mezache and H. Oudira, “ Radar CFAR detection in Weibull clutter based on zlog(z) estimator“, Remote Sensing Letters, Taylor&Francis, Vol. 11, no.6, pp.581-586, 2020.

[8] G. V. Weinberg, L. Bateman and P. Hayden, “Constant false alarm rate detection in Pareto type II clutter”, Digital Signal Processing, Vol. 68, pp. 192-198, 2017.

[9] V. G. Weinberg, S. D. Howard and C. Tran, “Bayesian framework for detector development in Pareto distributed clutter”, IET Radar Sonar & Navigation, Vol. 13, no. 9, pp. 1548-1555, 2019.

[10] A. Gouri, “Modeling, estimation and CFAR detection in non-Gaussian clutter” Phd Thesis, Department of Electronics, University of Mohamed Boudiaf Msila, 2020.

[11] S. Haykin, ‘‘*Adaptive Radar Signal Processing’’*, John Wiley, New Jersey, 2007.

[12] IPIX database. Available: http://soma.ece.mcmaster.ca/ipix/ipixspecs.html